

RESEARCH

Open Access



# PRAF2 as a novel biomarker for breast cancer with machine learning and experimentation validation

Zheng Wang<sup>1†</sup>, Zilin Bi<sup>1†</sup>, Hongguang Bo<sup>1†</sup>, Junyi Xu<sup>2†</sup>, Rui Sha<sup>1</sup>, Zhaocai Yin<sup>1</sup>, Changsheng Yu<sup>1</sup>, Yufa Xu<sup>1</sup>, Xiaomeng Shi<sup>1</sup>, Wenbo Song<sup>3</sup>, Bin Chen<sup>1</sup>, Yabing Wang<sup>1\*</sup>, Qian Zhang<sup>4\*</sup> and Jianping Chen<sup>1\*</sup>

## Abstract

**Background** Breast cancer (BC) is the most prevalent malignancy in women. Potential therapeutic targets for BC are of great significance. In our previous study, we found that prenylated rab acceptor 1 domain family member 2 (PRAF2) is an oncogene in BC. However, the exact mechanism of PRAF2 in BC cancer promotion is still not fully understood.

**Methods** Pan-cancer analysis of PRAF2 was performed in the TIMER, Kaplan–Meier, UALCAN and GEPIA databases. The prognostic value of PRAF2 in BC was investigated in the GEPIA database. The influence of PRAF2 on immune infiltration in BC was analyzed in the TISIDE and TIMER databases. Finally, we validated the expression of PRAF2 in our institutional samples. After downregulating PRAF2 in two BC cell lines, we tested cell proliferation by CCK-8 and Wound healing assays.

**Results** PRAF2 was highly expressed in various cancers, including BC, and in most BC cell lines. Higher expression of PRAF2 indicated poorer overall survival (OS) but not disease-free survival (DFS). Higher expression of PRAF2 is an independent prognostic factor in BC. PRAF2 is more highly expressed in BC than in the corresponding normal tissues. Downregulation of PRAF2 in BC can significantly inhibit viability and migration.

**Conclusions** PRAF2 is highly expressed in various cancers, including BC. The expression of PRAF2 is related to Liquid–Liquid Phase Separation in BC. Finally, PRAF2 is upregulated in BC based on our institutional data. Downregulation of PRAF2 significantly inhibits cellular viability and migration in BC. PRAF2 may be a potential biomarker and therapeutic target for BC.

**Keywords** PRAF2, Breast cancer, Molecular target, Immune infiltration, Novel biomarker

<sup>†</sup>Zheng Wang, Zilin Bi, Hongguang Bo and Junyi Xu contributed equally to this work.

\*Correspondence:

Yabing Wang  
wangeb3@wnmc.edu.cn  
Qian Zhang  
qianzhang90@163.com  
Jianping Chen  
chenjianping2023@126.com

<sup>1</sup> Department of Thyroid and Breast Surgery, Yijishan Hospital, First Affiliated Hospital of Wannan Medical College, Zhesan West Rd No. 2, Wuhu, Anhui Province 241001, China

<sup>2</sup> School of Basic Medical Science, Capital Medical University, No. 10 Right Outside the Western Headlines, Beijing 100069, China

<sup>3</sup> Department of Oncology, Jiangdu People's Hospital Affiliated to Medical College of Yangzhou University, 9 Dongfanghong Road, Jiangdu District, Jiangsu Province, Yangzhou 225299, China

<sup>4</sup> Department of Epidemiology and Health Statistics, School of Public Health, Fujian Medical University, University Town, Xue Yuan Road 1, Fujian Province, Fuzhou 350122, China



© The Author(s) 2025. **Open Access** This article is licensed under a Creative Commons Attribution-NonCommercial-NoDerivatives 4.0 International License, which permits any non-commercial use, sharing, distribution and reproduction in any medium or format, as long as you give appropriate credit to the original author(s) and the source, provide a link to the Creative Commons licence, and indicate if you modified the licensed material. You do not have permission under this licence to share adapted material derived from this article or parts of it. The images or other third party material in this article are included in the article's Creative Commons licence, unless indicated otherwise in a credit line to the material. If material is not included in the article's Creative Commons licence and your intended use is not permitted by statutory regulation or exceeds the permitted use, you will need to obtain permission directly from the copyright holder. To view a copy of this licence, visit <http://creativecommons.org/licenses/by-nc-nd/4.0/>.

## Introduction

Breast cancer (BC) is the most common malignancy in women, with approximately 600 thousand new diagnoses and 100 thousand deaths worldwide [1, 2]. Despite the fact that the mortality rate of breast cancer is decreasing, advanced stage breast cancer is still a tricky problem worldwide, and the 5-year survival rate of stage 4 ranges from 28%–32% [3]. Early diagnosis and novel therapeutic targets for breast cancer are of great significance. In the last decade, many novel therapeutic targets for breast cancer have been discovered. For example, atezolizumab for late-stage triple-negative breast cancer (TNBC) showed promising outcomes.

Prenylated rab acceptor 1 domain family member 2 (PRAF2) is from the Prenylated Rab acceptor family, comprising a four transmembrane domains, highly expressed in the endoplasmic reticulum (ER) [4–6], in recent studies, PRAF2 was associated with poorer prognosis in esophageal squamous and hepatocellular cancer [7, 8]. In our previous study, we found that prenylated rab acceptor 1 domain family member 2 (PRAF2) is highly expressed in BC and acts as an oncogene to promote the proliferation and invasion of BC [9]. However, the underlying mechanism of PRAF2 in BC is not fully understood. In the present study, we aimed to perform a pancancer analysis of PRAF2 and to elucidate the cellular biofunction of PRAF2 in BC in vitro.

## Methods and materials

### Gene expression analysis

To examine the distinct expression patterns of PRAF2 in pancancer and nearby normal tissues, TIMER2.0 (<http://timer.cistrome.org>), Kaplan–Meier (KM) Plotter database (<http://kmplot.com/analysis/>), GEPIA database (<http://gepia2.cancer-pku.cn/#analysis>), and UALCAN (<https://ualcan.path.uab.edu/>) were utilized. The levels of gene expression were displayed on a log<sub>2</sub> (TPM + 1) scale, with TPM representing transcripts per million. The expression of PRAF2 in breast cancer was analyzed using the XIANTAO platform (<https://www.xiantao.love/>) to compare BC with paired normal tissue in human cancers. The Human Protein Atlas (<https://www.proteinatlas.org/>) provides transcriptomic and proteomic data of human cells, tissues, and organs obtained from both healthy and diseased tissues using RNA sequencing (RNA-Seq) analysis and immunohistochemistry (IHC). The HPA database (<https://www.proteinatlas.org/>) analyzed the expression of PRAF2 in numerous cell lines, including leukemia, lung, breast, and brain cell lines, using the search term PRAF2. The HPA database was used to perform additional verification of the strength of PRAF2 immunohistochemical staining in various cancer tissues, particularly in breast

carcinoma. Furthermore, the HPA database was utilized to investigate the intracellular localization of PRAF2 in neoplasms [10].

### Analysis of the correlation between PRAF2 and clinicopathological parameters of BC

UALCAN, as mentioned before, is a web tool that offers a comprehensive and interactive analysis of bioinformatics. It utilizes RNA-seq and clinical information from TCGA to study 31 different types of malignancies [11]. We utilized UALCAN to examine the expression of PRAF2 and its association with different clinicopathological factors (such as cancer stage, age, subtype, menopause status, nodal metastasis status, and TP53 mutation status) in BC.

### Analysis of the prognostic value of PRAF2 in BC

To investigate the prognostic significance of PRAF2 expression in BC [12], the GEPIA database (<http://gepia2.cancer-pku.cn/#analysis>) and Kaplan–Meier plotter database (<http://kmplot.com/analysis/>) were utilized. The XIANTAO platform was utilized to generate an ROC curve for assessing the prognostic model intensity prediction accuracy. In our investigation, we utilized the GEPIA repository to examine the association between PRAF2 expression and both overall survival (OS) and disease-free survival (DFS) in BC. Based on a threshold of 50%, the TCGA tumor samples were categorized into cohorts of high-expression and low-expression. Through utilization of the Kaplan–Meier Plotter database, a correlation was discovered between the expression of PRAF2 and overall survival (OS) as well as relapse-free survival (RFS) in individuals with BC. Additionally, data comes from databases and the results have corrected for these confounding factors. The hazard ratio (HR) was estimated along with its 95% confidence intervals, and the *p* value for log-rank test was also calculated. A *p*-value less than 0.05 was used to determine statistical significance.

### Analysis of gene mutations in PRAF2

cBioPortal (<https://www.cbioportal.org/>) is an online platform designed to analyze the genomic features of tumors in the PRAF2 gene [13]. Using the database, we conducted an analysis of the mutation frequency of PRAF2 across various types of cancer. The mutation alterations included mutation, amplification, and deep deletion.

### liquid–liquid phase separation (LLPS) analysis of PRAF2

Determining whether a protein sequence contains disordered regions is crucial when studying protein phase separation, as proteins with such regions are more likely to undergo phase separation. The Disordered Protein

Prediction Database can be accessed at <https://d2p2.pro> [14]. It can predict disordered regions of proteins encoded throughout the entire genome. Professor Robert B. Russell from the European Molecular Biology Laboratory in Germany initially created the PONDR (Predictor of Natural Disordered Regions) database, which can be accessed at <https://www.pondr.com/> [15]. We using two database predict disordered areas of PRAF2 protein.

#### **Immune cell infiltration with the tumor immune estimation resource (TIMER2.0) and the TISIDB database analysis**

TIMER2.0, also known as the Tumor Immune Estimation Resource, is an online platform that allows for the comprehensive analysis of immune infiltration in different types of cancers. It can be accessed at <https://timer.cistrome.org/> and has been described in reference [16]. Using correlation modules in TIMER2.0, the association between PRAF2 expression and gene markers of tumor-infiltrating lymphocytes (TILs), such as markers of CD8<sup>+</sup>/CD4<sup>+</sup> T cells, B cells, natural killer (NK) cells, cancer-associated fibroblasts, macrophages, and neutrophils, was examined. The TISIDB database is a web-based repository portal that gathers numerous datasets on human cancer from the TCGA database [17], accessible at (<http://cis.hku.hk/TISIDB/index.php>). In the TISIDB database, the relationship between the abundance of TILs and the expression of PRAF2 was examined. Expression dispersion maps were generated for a specific set of genes in BC by utilizing correlation modules. The TISIDB database was used to investigate the associations between PRAF2 expression and the immune or molecular subtypes of BC. Differences with a *P* value < 0.05 were considered statistically significant.

#### **Single-cell sequencing**

Cancer SEA (<http://biocc.hrbmu.edu.CancerSEA>) is a unique database for single-cell sequencing, offering diverse functional states of cancer cells at the single-cell level [18]. The analysis involved examining the correlation between the expression of PRAF2 and various tumor functions using single-cell sequencing data. T-SNE diagrams were utilized to exhibit the expression patterns of PRAF2 in individual cells within TCGA specimens.

#### **Protein–protein interaction network construction**

The website of BioGRID, the Biological General Repository for Interaction Datasets [19] is a website that allows users to create a protein–protein interaction network (PPI), which stands for protein–protein interaction, and serves as a public repository for storing and sharing genetic and protein interaction information from both model organisms and humans. The PPI of PRAF2 in BC was constructed using BioGRID.

#### **Gene enrichment analysis**

The top 100 genes correlated with PRAF2 were obtained from all tumor and normal tissues in TCGA using GEPIA2.0. Next, we performed a correlation analysis using the Pearson method to examine the relationship between PRAF2 and the chosen genes. In order to examine the biological functions and signaling pathways influenced by PRAF2 in TCGA tumors, the XIANTAO platform was utilized for conducting Gene Ontology (GO) and Kyoto Encyclopedia of Genes and Genomes (KEGG) enrichment analyses. *p* value < 0.05 was considered to be statistically significant. Furthermore, we integrated the two sets of data to undertake KEGG pathway analysis. The DAVID bioinformatics database is a visual tool utilized for investigating the gene expression pattern through the website <https://david.ncicrf.gov/> [20]. By employing gene set enrichment analysis (GSEA), we utilized DAVID database to investigate the Gene Ontology biological process (GO-BP), Gene Ontology cellular component (GO-CC), Gene Ontology molecular function (GO-MF), and KEGG pathways associated with PRAF2 and its co-expressed genes.

#### **Cell culture and transfection**

The MDA-MB-231 and BT-549 breast cancer cell lines, along with the MCF-10A human normal mammary epithelial cell line, were acquired from The Cell Bank of Type Culture Collection of The Chinese Academy of Sciences. Additionally, the MCF-7 cell line (cat. no. CL-0149) was acquired from Procell Life Science & Technology Co., Ltd. All cell lines were cultured using high-glucose DMEM (cat. no. SH30022.01; Cytiva) with the addition of 10% FBS (cat. no. S711-001S; Shanghai Shuangru Biotechnology Co., Ltd.). The experiment was conducted at a temperature of 37 degrees Celsius and with a carbon dioxide concentration of 5%. The Lentivirus-si-PRAF2 was acquired from GenePharma located in Shanghai, China. Lentiviruses were ultracentrifuged, concentrated, and validated. Cells that had undergone transfection were chosen using puromycin (Solarbio, Beijing, China) for a duration of 7 days. The remaining cells were utilized as steady mass transfectants, consisting of three siRNA sequences that target PRAF2 and a negative control (NC) sequence, namely siRNA1, siRNA2, siRNA3, and siRNA-NC. Table 1 contains the siRNA sequences. Cell transfection was performed using Lipofectamine® 2000 (Invitrogen; Thermo Fisher Scientific, Inc.). Prior to transfection, MDA-MB-231, MCF-10A, BT-549, and MCF-7 cells were placed in 24-well plates with an optimized density of  $1 \times 10^5$  cells per well, 24 h in advance. The next day, once the cells had reached a confluence of 60–70%, PRAF2 siRNA (10  $\mu$ l/well) or siRNA-NC (10

**Table 1** The LVshRNA sequences

Product number	Product name	Position	Target sequence (5'–3')
R2023-SH1515	shRNA1	513	ACTAGAGGCACTGGG ACAAGA
R2023-SH1516	shRNA2	140	TCTACTACCAACCA ACTACC
R2023-SH1517	shRNA3	456	CAAGATTGAGAACAA GATCGA
R2023-SH1518	LV16NC	0	TTCTCCGAACGTGTC ACGT

μl/well) were transfected with 1 μl Lipofectamine 2000 reagent at room temperature for 48 h, with a final concentration of 100 nM. The manufacturer's protocol was followed, and medium was added to each well after 6 h of transfection. After transfection, cells were subjected to subsequent assays to evaluate cellular function. The siRNA with the highest transfection efficiency, as determined by analyzing PRAF2 protein expression 48 h post-transfection, was used for these assays.

#### Immunohistochemistry (IHC)

The analysis included tissue samples from 40 BC cases with pathological diagnosis that were treated at the Department of Thyroid and Breast Surgery, Yijishan Hospital of Wannan Medical College (Wuhu, China) from October 2021 to October 2022 were included in the analysis. Before the surgery, none of the patients had undergone neoadjuvant chemotherapy, radiotherapy, or endocrine treatment, who were informed of the objective of the study and gave informed consent. This research received approval from the Ethics Committee of Yijishan Hospital, affiliated with Wannan Medical College in (Wuhu, China) (No. 202325). The specimens were preserved in formaldehyde and treated with heat-induced antigen retrieval in citrate buffer (pH=6). The samples were subsequently obstructed and cultured with rabbit polyclonal anti-PRAF2 (1:500, cat. no. ab230420; Abcam). The sample was incubated with the primary antibody overnight at a temperature of 4 °C. The Elivision™ plus Polymer HP (Mouse/Rabbit) IHC Kit (Cat. KIT-9901, MXB Biotechnologies, China) has been developed. The

staining intensity was evaluated by two pathologists who were not aware of the clinical outcome.

#### Western blotting

Cold PBS was used to wash the tissue samples, which were then lysed using PhosphoSafe™ Extraction Reagent (cat. no. P0013; Beyotime Institute of Biotechnology). Before rinsing the cells with PBS, the culture medium was removed from the cells. To begin, the suggested quantity of Phospho Safe™ Extraction Reagent was introduced. Following this, the cultures were left to incubate at room temperature for a duration of 5 min. Next, the cells were detached using a cell scraper and the resulting lysate was moved to a 1.5 ml tube. Finally, the lysate was subjected to centrifugation at 16,000×g for 5 min at a temperature of 4 °C. Finally, the liquid above the sediment was moved to a fresh tube, and the amount of protein was measured using a BCA assay (cat. no. AS1086; Wuhan Aspen Biotechnology Co., Ltd.). Each sample total protein loading was adjusted to 30 μg, followed by electrophoresis using 15% SDS-PAGE and subsequent transfer to a PVDF membrane. To prevent non-specific binding in membranes, a solution of PBS with 5% nonfat milk was applied for 2 h at room temperature. Afterwards, the membranes were exposed to primary antibodies overnight at a temperature of 4 °C. The membranes were subsequently cultured with an HRP-linked goat anti-rabbit IgG (1:5,000; cat. no. BL103A; Micro Biotechnology (Shanghai) Co., Ltd.) was incubated at room temperature for 2 h. In the end, protein bands were identified by utilizing an improved chemiluminescence kit (cat. no. A38555; Thermo Fisher Scientific, Inc.). In this study The following antibodies were used in the present study: GAPDH (1:5,000; cat. no. ab37168; Abcam), PRAF2 (1:3,000; cat. no. ab230420; Abcam), Bax (1:1,000; rabbit.A0207; ABclonal), Bcl-2 (1:1,000; rabbit. no.A0208; ABclonal).

#### Reverse transcription-quantitative PCR (RT-qPCR)

A QuantiNova™ SYBR Green PCR kit was used for this assay (cat. no. 208252; Qiagen AB). The primers for the PRAF2 and GAPDH genes were synthesized by Guangzhou RiboBio Co. Ltd., and their sequences are detailed in Table 2. TRIzol® reagent (Invitrogen; Thermo Fisher Scientific, Inc.)

**Table 2** The primer sequences for q-PCR

Product number	Product name	Primer sequences (5'–3')
GQP0005157	geneDETECTTM hPRAF2_qPCR_91bp_F1	CCCAGGTCAAGACATTGCC
GQP0005158	geneDETECTTMhPRAF2_qPCR_91bp_R1	GGTCCAACAGTCAGGATACCC
ssD1021	GAPDH_2_Forward Primer(h,m,r)	GAACGGGAAGCTCACTGG
ssD1022	GAPDH_2_Reverse Primer(h,m,r)	GCCTGCTTCAACACCTTCT



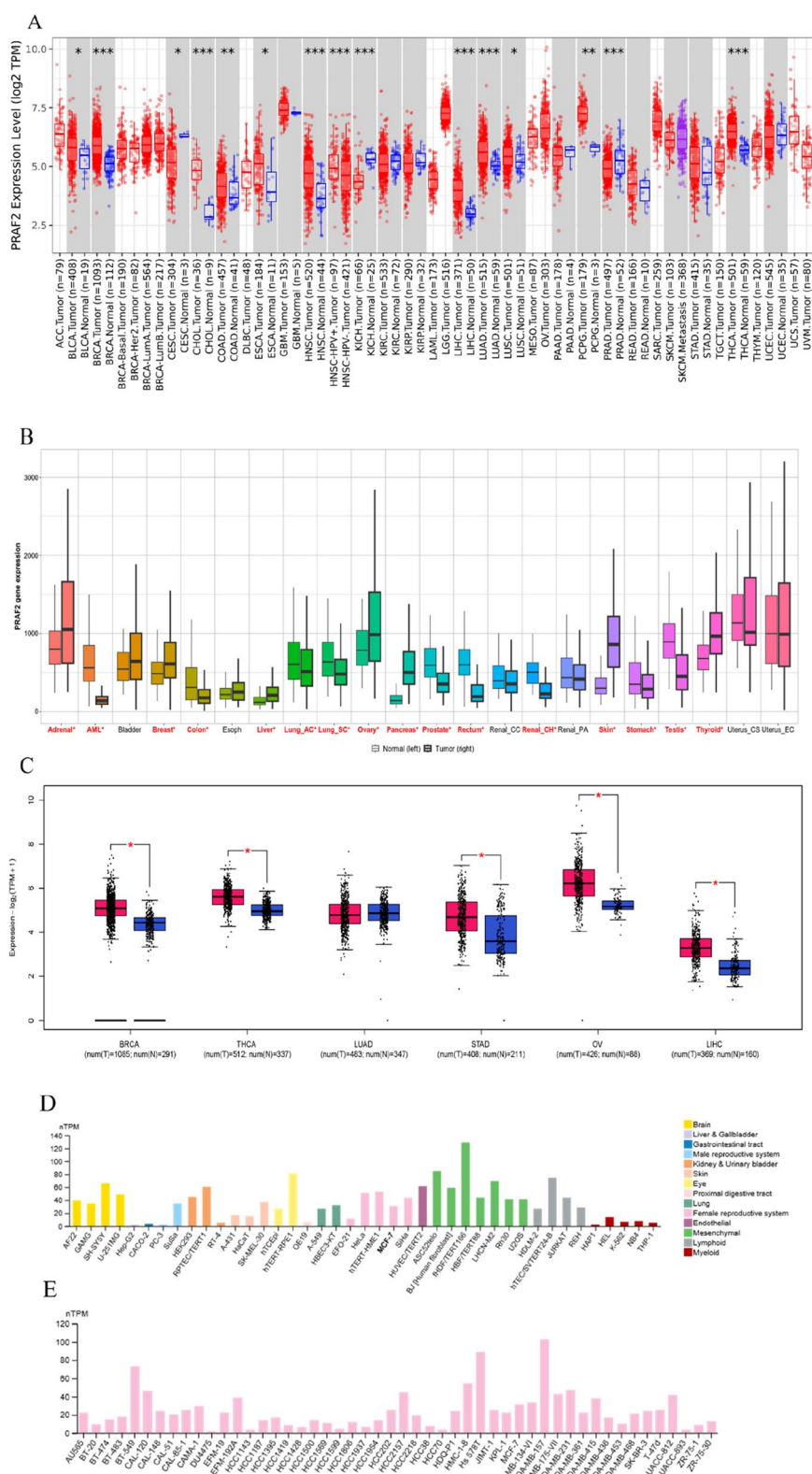


**Fig. 1** The expression of PRAF2 in pan-cancer. **A** Expression levels of PRAF2 in various types of cancers obtained from TIMER2.0. **B** PRAF2 expression in different cancers from KM-plotter database. Red script represents difference is significant. **C** PRAF2 expression in various cancer tissues and normal tissues analyzed by GEPIA. **D, E** PRAF2 expression in different cancer cell lines and breast cancer cell Lines, analyzed by HPA. \* $p < 0.05$ ; \*\* $p < 0.01$ ; \*\*\* $p < 0.001$

was used to extract total RNA from tissue samples and transfected cells, in accordance with the manufacturer's protocol. The RNA was converted into cDNA by utilizing the PrimeScript™ RT Reagent Kit with gDNA Eraser (cat. no. RR047A; Takara Bio, Inc.). Following the guidelines provided by the manufacturer, Takara Bio, Inc. performed the experiment. The QuantiNova™ SYBR Green PCR kit (cat. no. 208252; Qiagen AB). using the ABI PRISM 7000 fluorescent quantitative PCR system (Applied Biosystems; Thermo Fisher Scientific, Inc.). The thermocycling process involved one cycle at a temperature of 94 °C for a duration of 3 min, followed by 35 cycles at the same temperature for 30 s, then at 58 °C for another 30 s, and finally at 72 °C for 45 s. The 2- $\Delta\Delta C_q$  method [21] was used to calculate the relative expression. The internal control was provided by GAPDH. The trial was conducted on three separate occasions.

#### Cell counting Kit-8 (CCK-8) assay

Cell proliferation capability was determined using the CCK-8 assay from (Beyotime Institute of Biotechnology), following the guidelines provided by the manufacturer. After adhering, cells in the phase of logarithmic growth (100  $\mu$ l) were placed onto a 96-well plate (10<sup>3</sup> cells/well), and subsequently, the culture medium was removed. Afterward, the cells were incubated with 10  $\mu$ l of CCK-8 reagent for a period of 72 h. As a negative control, the culture medium without cells was utilized and subsequently incubated with the CCK-8 reagent. To determine the MCF-7 and BT549 cell proliferation rate, the microplate reader was utilized to measure the absorption of each well at 450 nm. This measurement included both the average value of each group of cells and the negative controls. The percentage of cell proliferation rate is calculated by dividing the value of each experimental group by the value of the NC control group and multiplying it by 100. The trial was conducted on three separate occasions.

#### Scratch wound healing assay

The transfected cells were cultured in six-well plates, and the monolayers were scraped longitudinally with a sterile 10- $\mu$ L pipette tip once the cells were 80% confluent. After rinsing the cell debris with PBS, the adherent cells were cultivated in serum-free medium, After 24 h of incubation, each group was photographed under the microscope and recorded as 24 h. Experiment was repeated three times.

#### Statistical analysis

Summary statistics were utilized to depict the fundamental attributes of the patients. Statistical principles were used to analyze the distinctions between qualitative variables and continuous variables, employing chi-squared test statistics, t tests, and analysis of variance (ANOVA). In order to reduce the I type of error, the Bonferroni correction method was used in pair-to-pair comparisons in ANOVA, and the significance level was equal to 0.05/ number of comparisons between groups. The Kaplan–Meier method was utilized to estimate survival and then compared among the various groups using the log-rank test. Statistical significance was determined for all the two-tailed tests conducted, with a *p*-value below 0.05.

#### Results

##### PRAF2 expression analysis across cancers

We examined the variation in PRAF2 expression between tumor and adjacent healthy tissues by utilizing RNA-seq data obtained from diverse cancer types in TCGA. Based on the TIMER database, the levels of PRAF2 expression show a notable rise in BLCA (bladder urothelial carcinoma), BC (breast invasive carcinoma), HNSC (head and neck cancer), LIHC (liver hepatocellular carcinoma), LUAD (lung adenocarcinoma), LUSC (lung squamous cell carcinoma), PCPG (pheochromocytoma and paraganglioma), and THCA (thyroid carcinoma) when compared to the surrounding healthy tissue. In contrast, the expression of PRAF2 mRNA was found to be reduced in CESC (cervical squamous cell carcinoma and endocervical adenocarcinoma) and KICH (kidney chromophobe), as shown in (Fig. 1A). In the meantime, we utilized the Kaplan–Meier plotter database. According to the data presented in (Fig. 1B), it was observed that the expression of PRAF2 was reduced in acute myeloid leukemia (LAML), colon adenocarcinoma (COAD), lung adenocarcinoma (LUAD), lung squamous cell carcinoma (LUSC), prostate adenocarcinoma (PRAD), rectum adenocarcinoma (READ), stomach adenocarcinoma (STAD), testicular germ cell tumors (TGCTs), and uterine carcinosarcoma (UCS). In the meantime, we discovered increased expression of PRAF2 in ACC (adrenocortical carcinoma), BC (breast invasive carcinoma), LIHC (liver hepatocellular carcinoma), OV

(See figure on next page.)

**Fig. 2** The different expression of PRAF2 in breast cancer. **A** The KM-plotter database shows a higher level of PRAF2 expression in breast cancer compared to normal tissues. **B** The UALCAN database was utilized to investigate the expression of PRAF2 in breast cancer. **C, D** Analysis of PRAF2 expression in breast cancer compared to normal tissues and 58 pairs of breast cancer tissues and adjacent normal tissues in the TCGA database. **E** PRAF2 protein levels in normal and breast cancer tissues were visualized by IHC in HPA. **F** The subcellular localization of PRAF2 in tumor cells was visualized by immunofluorescence in HPA database. \*\*\**p* < 0.001

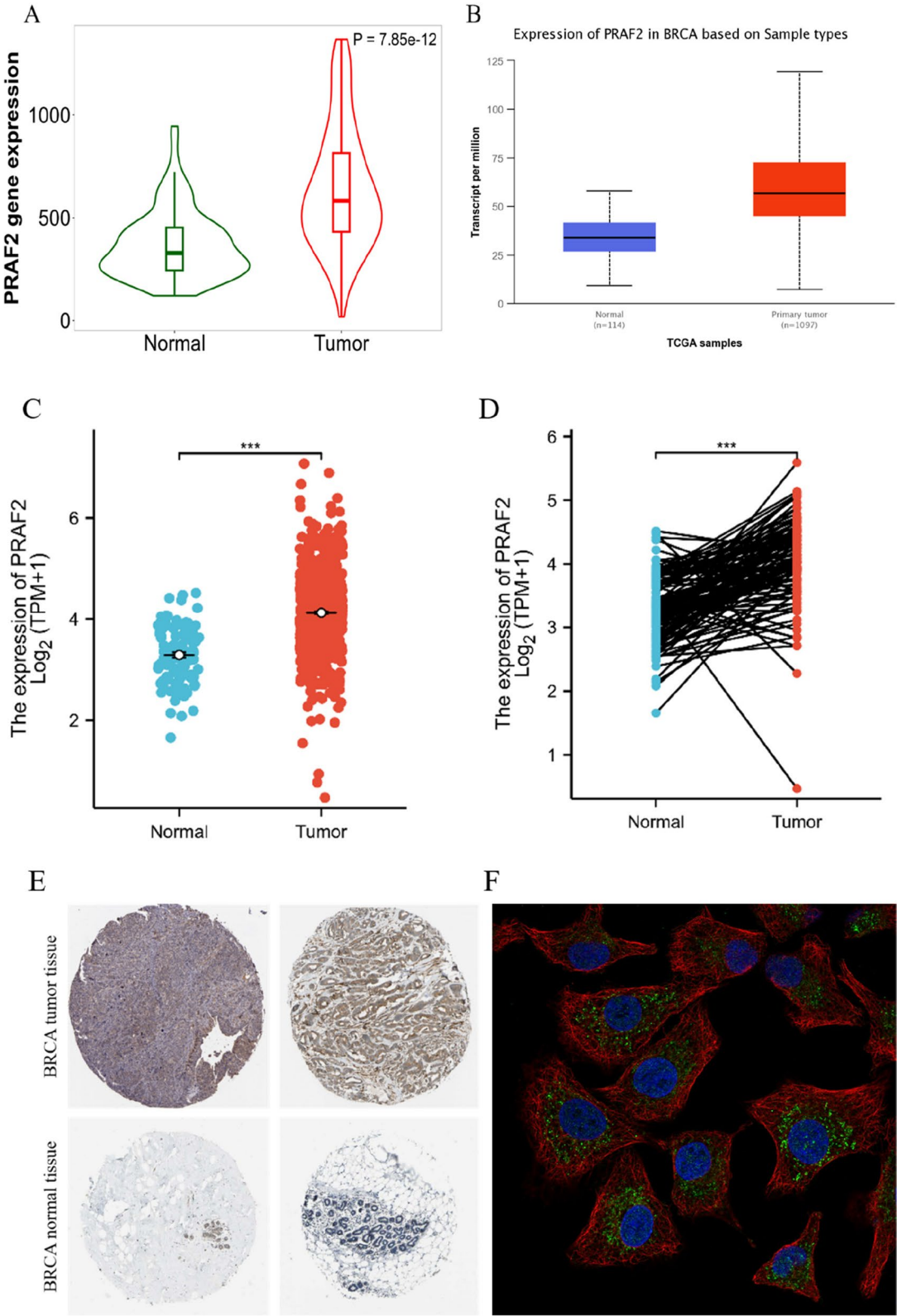


**Fig. 2** (See legend on previous page.)

(ovarian serous cystadenocarcinoma), PAAD (pancreatic adenocarcinoma), skin cancer, and THCA (thyroid carcinoma). In addition, we utilized GEPIA2.0 to investigate the expression level of PRAF2 in different types of cancers. Our findings revealed a significant increase in PRAF2 expression among individuals diagnosed with BC, THCA, STAD, OV, and LIHC. However, no such elevation was observed in patients with LUAD (Fig. 1C). In order to clarify the importance of PRAF2 expression in BC cells, we examined the levels of PRAF2 expression using RNA-Seq data retrieved from cell lines documented in HPA databases. (Fig. 1D–E) displayed elevated PRAF2 mRNA expression levels in BC cell lines including MCF7, MDA-MB-157, MDA-MB-231, and BT549.

### PRAF2 expression analysis in BC

The analysis conducted using the Kaplan–Meier plotter database, UALCAN online tool, and the XIANTAO platform revealed a significant increase in PRAF2 expression levels in BC (Fig. 2A–D). Additionally, we validated the expression of PRAF2 by utilizing the IHC findings obtained from the HPA database. In the BC study, immunohistochemical staining revealed that PRAF2 exhibited predominantly positive expression in the tumor tissue (Fig. 2E). In general, we exhibited elevated PRAF2 levels in breast cancer. Furthermore, the HPA database unveiled that PRAF2 exhibited both cytoplasmic and nuclear localizations (Fig. 2F).

### PRAF2 expression and clinical parameters of BC

We explored the expression of PRAF2 among patient groups based on various clinical parameters using the UALCAN online tool. In relation to the stage of the tumor, breast cancer patients in stages 1, 2, 3, and 4 showed a notable rise in the expression of PRAF2 (Fig. 3A). The PRAF2 level in breast cancer tissues of patients from various age groups (21–40 years, 41–60 years, 61–80 years, and 81–100 years) showed a significant increase, as depicted in (Fig. 3B). PRAF2 expression was markedly increased in luminal, Her-2-positive, and triple negative breast cancer specimens in comparison to the corresponding normal controls, as indicated by the subtype analysis (Fig. 3C). PRAF2

expression was elevated in breast cancer patients categorized as premenopause, perimenopause, and postmenopause based on their menopause status (Fig. 3D). PRAF2 expression was elevated in breast cancer patients categorized as N0, N1, N2, and N3 based on node metastasis status (Fig. 3E). Furthermore, an increase in PRAF2 expression was detected in breast cancer patients with both TP53 mutations and TP53 wild-type, when compared to normal controls (Fig. 3F). The findings indicate a strong association between the expression of PRAF2 and the advancement and spread of tumors. The calculated *P* value between each group was listed in Supplementary Table S1.

### The predictive significance of PRAF2 in terms of survival

In the GEPIA analysis, it was observed that increased PRAF2 levels were linked to decreased overall survival (OS) but did not affect disease-free survival (DFS) in BC patients ( $n = 1071$ , OS HR = 1.5,  $P = 0.028$ ;  $n = 1071$ , DFS HR = 1.1,  $P = 0.78$ ) (Fig. 4A, B). The Kaplan–Meier plotter database showed that increased PRAF2 expression was linked to worse OS but not DFS in BC. Specifically, the study found that higher PRAF2 expression was associated with a higher risk of mortality (OS (060831)  $n = 65$ , HR = 3.08,  $P = 0.0019$ ), while no significant association was observed with DFS (203,456)  $n = 63$ , HR = 1.55,  $P = 0.31$ ) (Fig. 4C, D). To assess the predictive accuracy of PRAF2 for BC overall survival (OS) and disease-specific survival (DSS), we utilized the time-dependent ROC curve. The results showed that PRAF2 had an AUC of 0.501, 0.654, and 0.739 for one-year, two-year, and three-year OS, respectively (Fig. 4E). Similarly, for DSS, the AUC values were 0.618, 0.695, and 0.739 for one-year, two-year, and three-year, respectively (Fig. 4F). The disease-free interval (DFI) had an area under the curve (AUC) of 0.540 for one year, 0.617 for two years, and 0.859 for three years, as shown in (Fig. 4G). The analysis of multiple variables indicated that PRAF2 could function as a standalone indicator for adverse results in BC cases. The aforementioned findings demonstrated a significant correlation between PRAF2 expression and the prognosis of BC.

(See figure on next page.)

**Fig. 3** The assessment of PRAF2 expression in various patient groups with breast cancer based on clinical parameters using the UALCAN database. **A** Box plot displays the comparative expression of PRAF2 in normal or patients with stage 1, 2, 3, or 4 breast cancers. **B** Box-plot displays the relative expression of PRAF2 in healthy subjects of any age and patients with breast cancer aged 21–40, 41–60, 61–80, and 81–100 years. **C** Box plot is presented to display the relative expression of PRAF2 in individuals with normal breast tissue and different molecular subtypes of breast cancer. **D** Box-plot illustrates the relative expression of PRAF2 in normal or patients with states of menopause breast cancers. **E** The box plot displays the comparative expression of PRAF2 in individuals without any abnormalities or patients with lymph node metastatic tumors. **F** Box-plot displays the comparative expression of PRAF2 in normal and breast cancer samples based on the TP53 status of patients



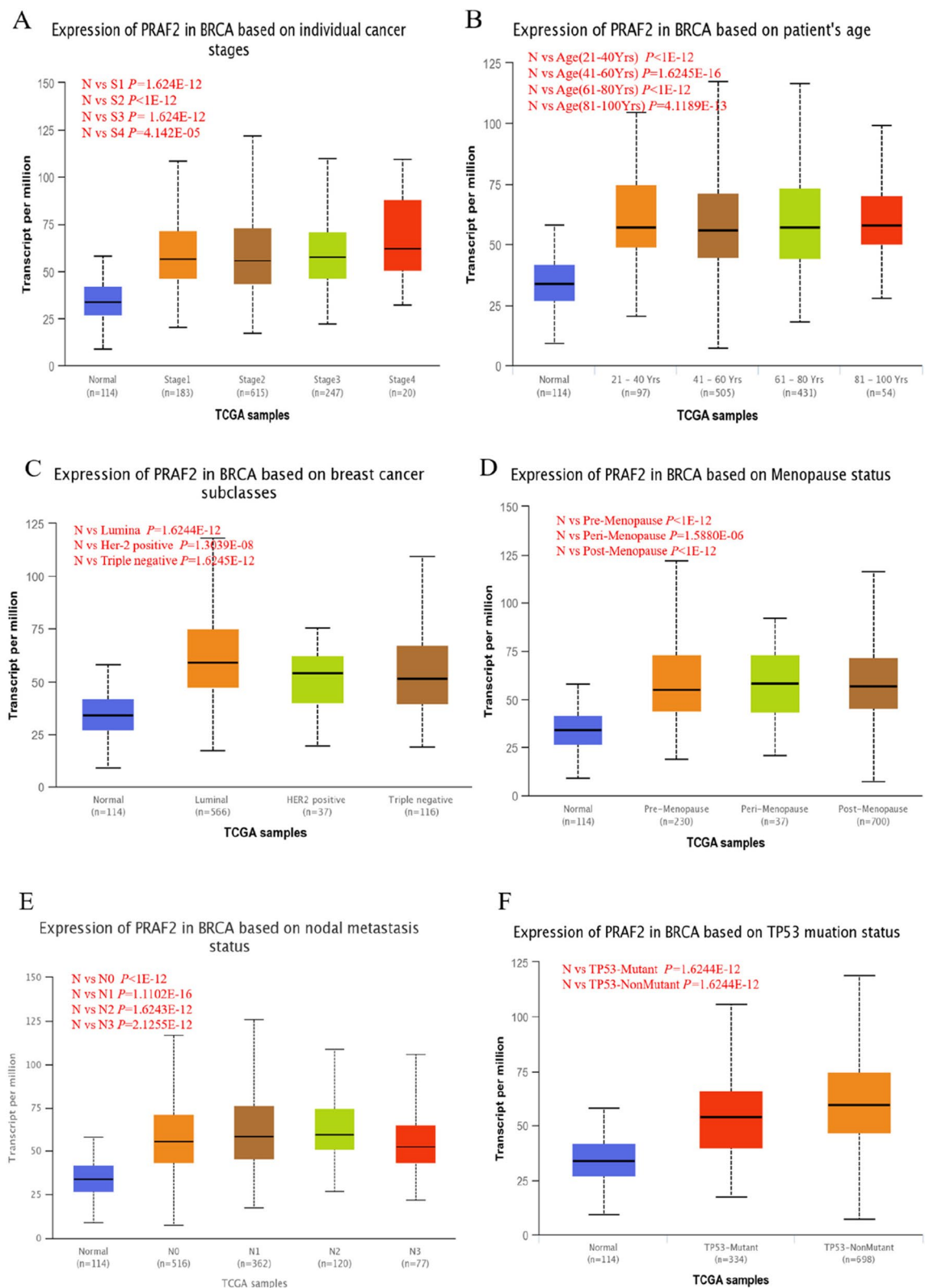


**Fig. 3** (See legend on previous page.)

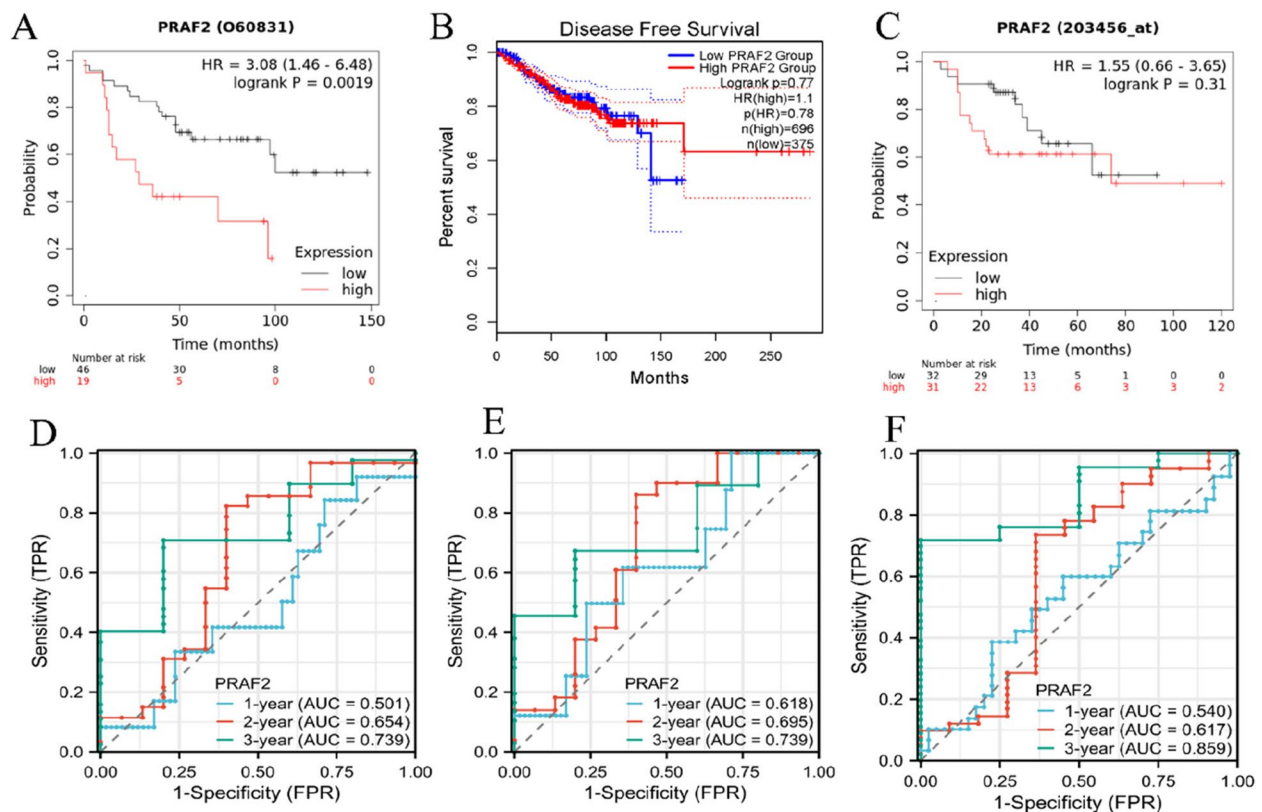


**Fig. 4** Assessing the predictive significance of PRAF2 levels in breast cancer. **A** Survival curves using the Kaplan–Meier plotter are shown for RFS. **B** Survival curves using the GEPIA2.0 are shown for DFS. **C** Survival curves using the Kaplan–Meier plotter are shown for OS. **D** The time-dependent ROC testified the predictive efficiency of PRAF2 for breast cancer OS. **E** The time-dependent ROC testified the predictive efficiency of PRAF2 for breast cancer DSS. **F** The time-dependent ROC testified the predictive efficiency of PRAF2 for breast cancer DFI

### Mutation analysis of PRAF2

The cBioPortal database was utilized to examine genetic changes in PRAF2 across various types of cancer. In ovarian epithelial tumor, the prevalence of genetic variation in PRAF2 was the highest at 5.66%, primarily in the form of mutation. Head and neck squamous carcinoma had the second highest occurrence rate of PRAF2 (3.85%), primarily as a mutation (Fig. 5A). Various alterations in the PRAF2 gene led to changes in copy numbers, as shown in (Fig. 5B).

### liquid–liquid phase separation (LLPS) analysis of PRAF2

The Disordered Protein Prediction Database offers a collection of forecasts that suggest the existence of disordered structural domains in PRAF2 (Fig. 6A). In the diagram, regions with PONDR scores above 0.5 are considered disordered, whereas regions with PONDR scores below 0.5 are considered ordered. By analyzing the sequence of the PRAF2 protein, we observed three regions of disorder (Fig. 6B). This indicates that PRAF2 is extensively disordered, implying the possibility of PRAF2 undergoing LLPS.

### Correlation between immune infiltration and PRAF2 expression in breast cancer

Tumor advancement is closely linked to the presence of immune infiltration. Hence, the utilization of TISIDB and TIMER platforms enabled the evaluation of the associations between PRAF2 expression and the levels of immune cell infiltration in BC. The presence of uncontaminated tumors in clinical cancer samples greatly affects the investigation of immune infiltration through genetic methods [22]. Hence, in this research, the expression of PRAF2 showed a positive correlation with the integrity of BC ( $\rho = 0.0766$ ,  $p < 1.62e-02$ ). The findings indicated a significant association between PRAF2 and the degree of tumor-infiltrating lymphocytes (TILs) infiltration. The high levels of PRAF2 expression showed a positive correlation with the infiltration degree of CD8+ T cells ( $\rho = 0.108$ ,  $p < 6.79e-04$ ), CD4+ T cells ( $\rho = 0.134$ ,  $p < 2.27e-05$ ), macrophages ( $\rho = 0.115$ ,  $p < 2.68e-04$ ), cancer-associated fibroblasts ( $\rho = 0.18$ ,  $p < 1.06e-08$ ), and NK cells ( $\rho = 0.15$ ,  $p < 6.21e-07$ ). Additionally, they exhibited a negative correlation with B cells ( $\rho = -0.2$ ,  $p < 2.16e-10$ ) and neutrophils

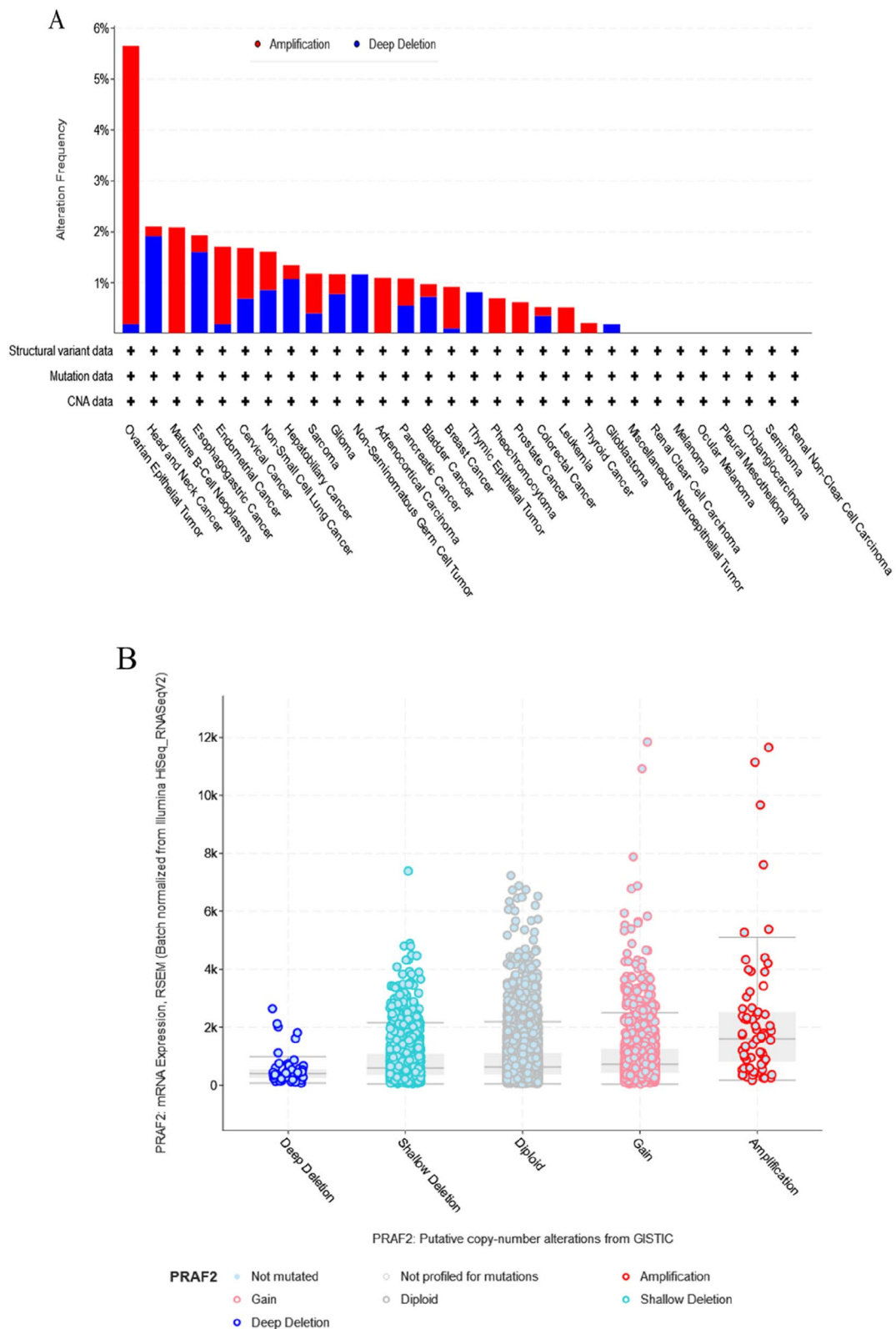


**Fig. 5** Genetic alterations of PRAF2 in pan-cancer using the cBioPort. **A** PRAF2 genomic alterations in pan-cancers analyzed by the cBioPortal database. **B** PRAF2 genomic alterations resulting in Copy number alterations

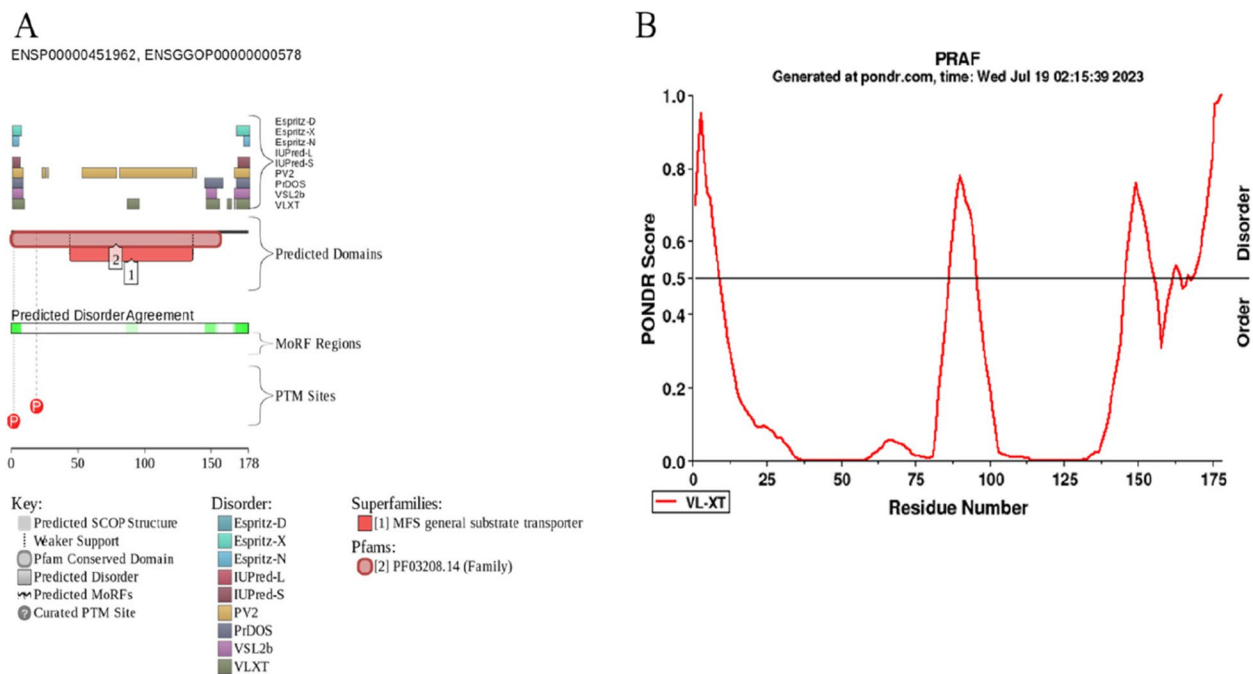


**Fig. 6** liquid-liquid phase separation (LLPS) Analysis of PRAF2 **A** Graph plotting disordered regions of PRAF2 using Database of Disordered Protein Prediction. **B** Graph plotting disordered areas of PRAF2 using POND

( $\rho = -0.12, p < 1.45e-4$ ) (Fig. 7A). Additionally, our findings demonstrated a significant association between PRAF2 and the prevalence of TILs (Fig. 7B). As an example, there was a strong positive correlation between it and the high presence of monocytes ( $\rho = 0.226, p < 4.35e-14$ ), while it showed negative correlations with activated CD4+ T cells ( $\rho = -0.176, p < 4.84e-09$ ), B cells ( $\rho = -0.243, p < 3.67e-16$ ), and Th2 cells ( $\rho = -0.249, p < 7.46e-17$ ). The  $p$ -values for all the tests were significantly below 0.001. The findings suggest that PRAF2 has a crucial function in the immune infiltration of BC.

#### PRAF2 expression is related to immune and molecular subtypes in breast cancer

Subsequently, the TISIDB website was utilized to investigate the involvement of PRAF2 expression in various immune and molecular subtypes of human cancers. There were six different types of immune subtypes that were classified, which are C1 (focused on wound healing), C2 (dominated by IFN-gamma), C3 (related to inflammation), C4 (depleted in lymphocytes), C5 (characterized by immunological quietness), and C6 (dominated by TGF- $\beta$ ). demonstrated that the expression of PRAF2 was associated with various immune subtypes in BC (Fig. 8A). PRAF2 expression did not vary between the groups for various molecular subtypes of cancers (Fig. 8B). After analyzing the aforementioned findings, we determined that the expression of PRAF2 varies among immune

subtypes but remains consistent among molecular subtypes of BC.

#### The single-cell expression pattern of PRAF2

In the Cancer SEA database, we conducted an analysis of PRAF2 at the single-cell level. In BC, the presence of PRAF2 showed a negative correlation with apoptosis and inflammation, while exhibiting a positive connection with epithelial-mesenchymal transition (EMT), hypoxia and stemness as shown in (Fig. 9A, B). Furthermore, the expression patterns of PRAF2 were visualized at the individual cell level in BC using a T-SNE diagram (Fig. 9C).

#### PRAF2 interaction network and functional analysis

To explore the potential interactions, we performed a PPI network analysis on the differentially expressed PRAF2. BioGRID provided a total of 19 molecules that interacted with PRAF2, as depicted in (Fig. 10A). Furthermore, we obtained the top 100 comparable PRAF2 genes (shown in Supplementary Table S2) in BC through GEPIA2.0. Perform GO and KEGG enrichment analyses as shown in (Fig. 10B). The findings suggested that the co-expressed genes of PRAF2 play a crucial role in the control of tumor formation and growth. Mitochondrial respiratory chain complex assembly was enriched in GO-BP, respiratory chain complex I in GO-CC, and NADH dehydrogenase activity in GO-MF. KEGG enrichment analyses in the



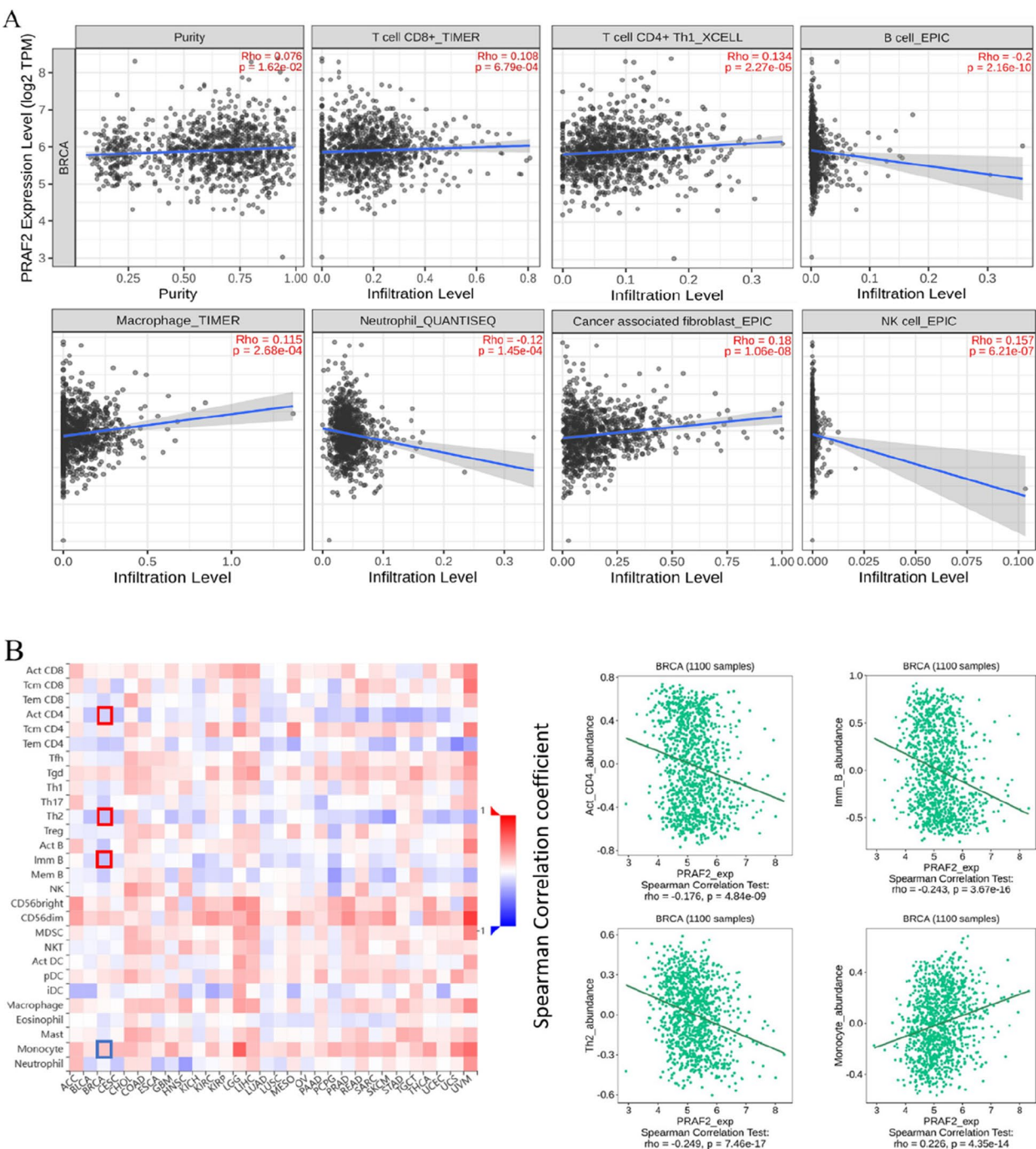


**Fig. 7** Association between immune infiltration and expression of PRAF2 in breast cancer. **A** The TIMER2.0 database provides information on the correlation between PRAF2 expression and the infiltration levels of CD8+T cells, CD4+T cells, B cells, macrophages, neutrophils, tumor-associated fibroblast cells, and natural killer cells in breast cancer. **B** The TISIDB database provides information on the correlation between the expression of PRAF2 and the abundance of tumor-infiltrating lymphocytes in breast cancer

neurodegeneration multiple disease pathway. Afterwards, the gene set enrichment analysis (GSEA) was employed to identify the primary GO terms associated with the co-expressed genes of PRAF2. Upon further examination, we

investigated the biological process classifications of GO and discovered that PRAF2 and its coexpressed genes predominantly engaged in governing the functionality of mitochondria ATP synthesis coupled proton transport,

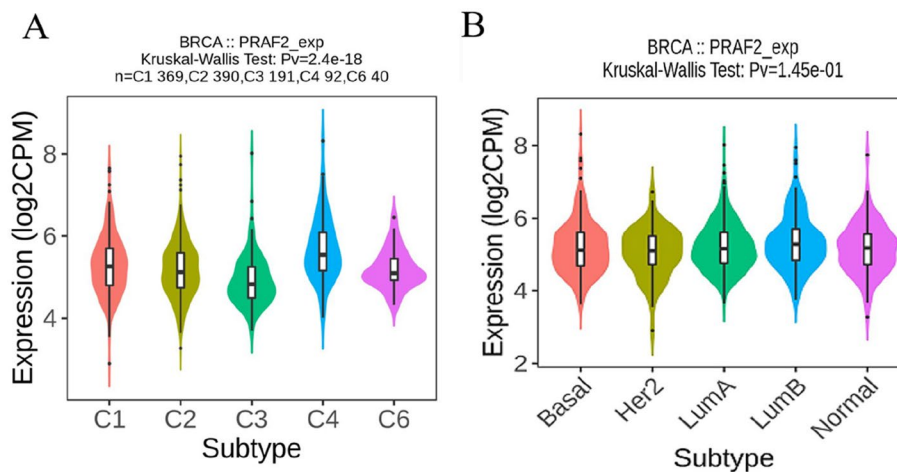


**Fig. 8** Correlation of PRAF2 expression with immune infiltration in breast cancer. **A** The relationship between PRAF2 expression and breast cancer immune subtypes. **B** The relationship between PRAF2 expression and breast cancer molecular subtypes

Mitochondrial respiratory chain I and ion transmembrane transporter activity as depicted in (Fig. 10C-E). Subsequently, we conducted KEGG pathway analysis and observed that co-expressed genes were significantly enriched in oxidative phosphorylation (Fig. 10F). These pathways are known to have a crucial impact on cancer metastasis and therapeutic resistance [23].

#### Validation of PRAF2 expression in BC

IHC staining was used to further examine the expression of PRAF2 in BC cases. The intensity of positive cells was graded as follows: 0, negative; 1, light yellow, weak; 2, yellow brown, moderate; or 3, brown, strong. In comparison to normal tissues (Fig. 11A, B), it was evident that the PRAF2 level exhibited a noticeable increase in BC tissues. In BC tissues, the level of PRAF2 expression was markedly elevated compared to normal adjacent tissues (Fig. 11C) showed that the mRNA and protein expression of PRAF2 was greater in the breast cancer cell lines MCF-7 and BT-549 compared to MCF-10A in vitro experiment (Fig. 11D,E). Therefore, MCF-7 and BT-549 were subsequently used for siRNA transfection to knock down the expression of PRAF2 protein. There were three siRNA used in further study, siRNA-NC group and siRNA-1, siRNA-2 and siRNA-3 group. Total protein from cells of each group was extracted after transfection, and the gene knockdown rate in the control group was detected by western blotting (Figs. 11F and 2G). The results showed that PRAF2 expression was decreased in cells transfected with siRNA-1-PRAF2 compared with siRNA-NC, showing superior knockdown efficiency. Therefore, siRNA-1 was selected for subsequent experiments.

#### Knockdown of PRAF2 inhibits BC cell progression and migration in vitro

We assessed the impact of PRAF2 on the survival of MCF-7 and BT-549 cells using the CCK-8 assay. According to the findings, the introduction of siRNA-PRAF2 resulted in a decreased growth rate of MCF-7 and BT-549 cells after 96 h in comparison to siRNA-NC cells (Fig. 12A). The findings suggested that a reduction in PRAF2 expression could reduce the survival of MCF-7 and BT-549 cells. A scratch test was used to investigate the effect of PRAF2 on the migration of MCF-7 and BT-549 cells. The results revealed that the migration of the siRNA-PRAF2 group was significantly reduced compared with siRNA-NC (Fig. 12B). This indicated that downregulation of PRAF2 in MCF-7 and BT-549 cells significantly suppressed cell migration in vitro experiment. As we mentioned earlier, PRAF2 was negatively associated with apoptosis, in our study, Cells transfected with siRNA-PRAF2-1 presented pro-apoptotic proteins Bax was significantly higher, whereas the anti-apoptotic protein Bcl-2 was significantly lower compared with those transfected with siRNA-NC ( $p < 0.05$ ) (Fig. 12C-E), indicating that downregulation of PRAF2 in breast cancer cells may affect the apoptosis.

#### Discussion

PRAF2 is an endoplasmic reticulum (ER) protein that participates in protein and vesicle transport from the ER to the Golgi [6]. Previous studies found that PRAF2 is upregulated in some tumors, such as neuroblastoma, esophageal squamous cell cancer and hepatocellular carcinoma [8, 24, 25]. However, no one has performed a pancancer analysis of PRAF2. In the present study, we

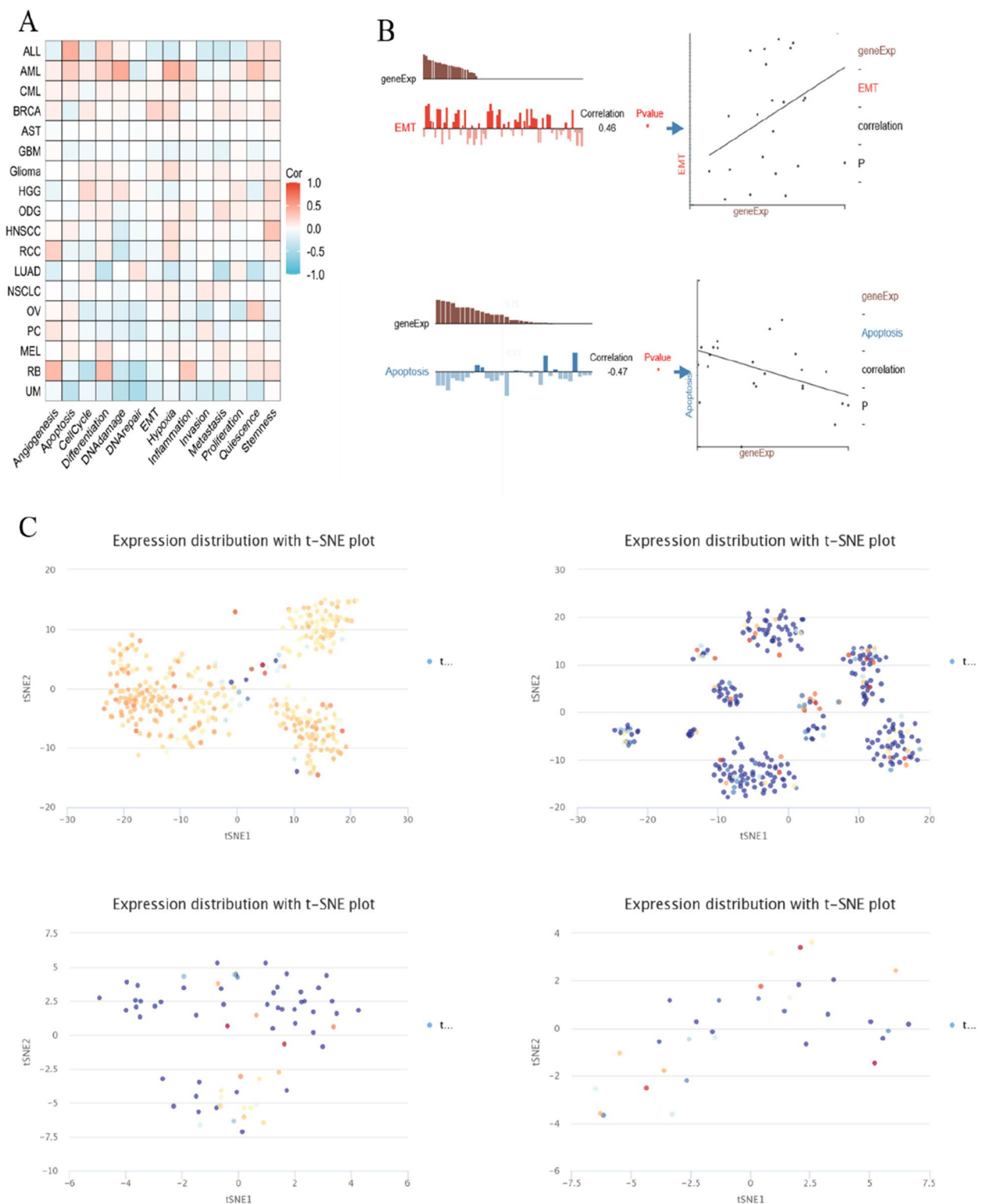


**Fig. 9** The association between expression levels of PRAF2 and functional states using single-cell sequencing datasets. **A** The CancerSEA tool was used to investigate the relationship between PRAF2 expression and different functional states in tumors. **B** relationship between expression of PRAF2 and EMT \ apoptosis. **C** The T-SNE diagram displayed the expression profiles were shown at single cells from BC

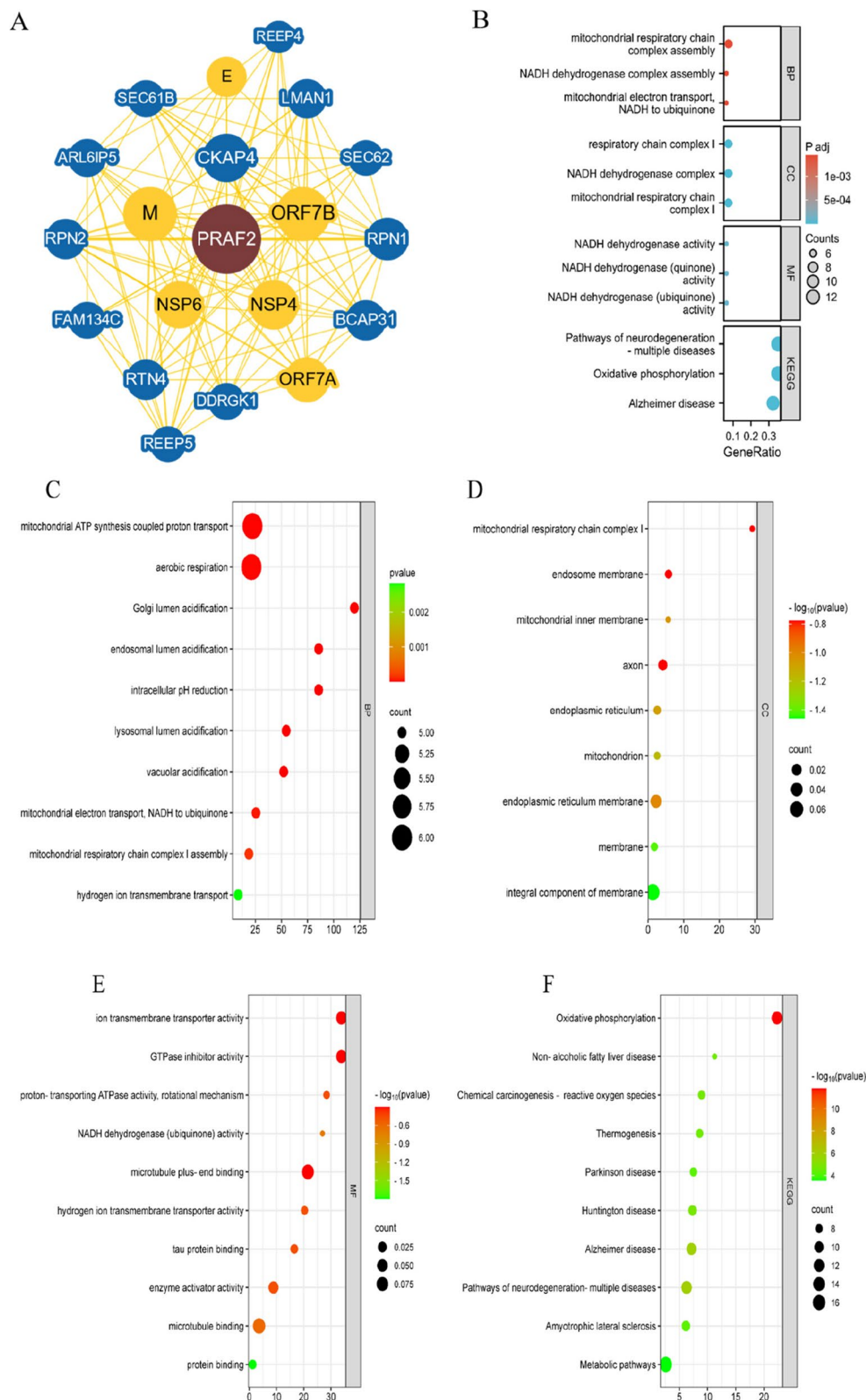


**Fig. 10** Functional enrichment analysis of PRAF2-related genes. **A** PRAF2-related genes were obtained from the Bio GRID web tool, and 19 proteins were displayed. **B** functional enrichment of PRAF2 co-expressed genes interactive network modules GO- Biological processes. Cellular components. Molecular functions, KEGG. **C-E** GO- Biological processes > Cellular components, Moecular functions of PRAF2 related gene analyzed by the DAVID bioinformatics database. **F** KEGG signal pathway analyzed by the DAVID bioinformatics database



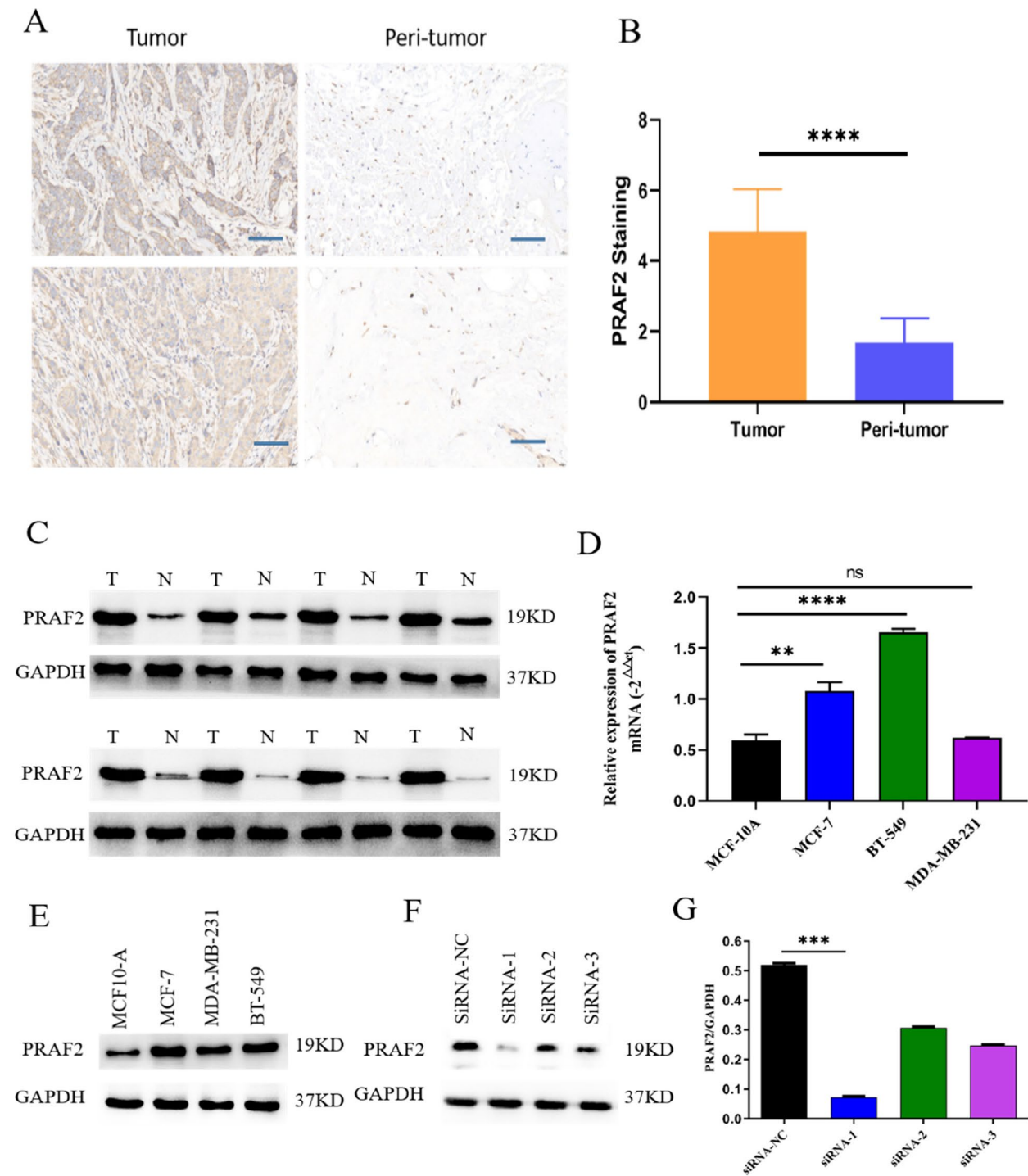


**Fig. 11** The expression of PRPF2 in cell lines and BC tissues and. **A** representative IHC staining patterns of PRPF2 in BC tissues and peritumor tissues. Scale bar was 20  $\mu$ m. **B** Quantitative analysis of protein expression of PRPF2 in tumor tissues and peritumor tissues by IHC staining ( $n=40$ ). **C** Representative images of western blots for the protein expression of PRPF2 in tumor (T) tissues and normal (N) tissues, as normalized to GAPDH. **D** The expression of PRPF2 in breast cancer cell lines MCF-10A, MCF-7, BT-549, MDA-MB-231 and was detected by q-PCR. **E** Representative images of western blots for the protein expression of PRPF2 in breast cancer cell lines MCF-10A, MCF-7, BT-549, MDA-MB-231, as normalized to GAPDH. **F** PRPF2 expression was in MCF-7 cells transfected with siRNA-PRPF2 detected by Western blot analysis. **G** Quantitative analysis of protein expression of PRPF2 was in MCF-7 cells transfected with siRNA-PRPF2 detected by Western blot analysis. \*\*  $p < 0.01$ , \*\*\*  $p < 0.001$ , \*\*\*\*  $p < 0.0001$

performed a comprehensive bioinformatic analysis of PRAF2 in various cancers, especially in BC. The analysis revealed the cancer-promoting effects of PRAF2 in BC and the related cellular function gene of PRAF2. Moreover, PRAF2 is associated with tumor immunity, which may be of great therapeutic potential in the future.

We analyzed the expression of PRAF2 in various cancers from several public databases and found that PRAF2 is highly expressed in various solid cancers. Previous studies have demonstrated that PRAF2 is significantly upregulated in neuroblastoma and is associated with oncological survival [26]. Furthermore, we found that PRAF2 is more highly expressed in BC samples than in the corresponding normal tissues. The results showed that PRAF2 is highly expressed in most BC cell lines, such as MCF7, MDA-MB-157, MDA-MB-231 and BT549, indicating that PRAF2 might function as an oncogene in BC. The HPA database showed the distribution of PRAF2 in both the cytoplasm and nucleus.

We conducted an analysis of PRAF2 and clinical characteristics. The results indicated that PRAF2 expression is associated with cancer stage, age, tumor subclasses, menopause status, metastasis status and TP53 mutation status. In the survival analysis, we found that high expression of PRAF2 was associated with poorer OS but not DFS in both the GEPIA and Kaplan–Meier plotter databases. The time-dependent ROC curve showed that the predictive efficiency of PRAF2 was best at three years for OS, DSS and DFI. Qian et al. conducted a study by analyzing 77 esophageal squamous cell carcinoma (ESCC) samples and found that PRAF2 was increased in ESCC. Survival analysis showed that high expression of PRAF2 was associated with poorer prognosis [25]. These results provide further proof of the cancer-promoting function of PRAF2 in BC.

In the last decade, immunotherapy has become the hottest topic in cancer treatment. Immune infiltration is closely related to tumor progression. Our results indicated that PRAF2 is positively correlated with tumor purity, CD8+T cells, macrophages, cancer-associated fibroblasts and NK cells and negatively correlated with B cells and neutrophils. The total abundance of TILs is reported to be associated with better prognosis in large

cohort studies [27, 28]. Oshi et al. reported that a higher proportion of CD8+T cells and CD4+T cells in triple-negative breast cancer (TNBC) indicated higher expression of immune checkpoint molecules, suggesting better outcomes with immune therapy [29]. Macrophages and cancer-associated fibroblasts have been proven to promote tumor progression in BC [30, 31]. PRAF2 expression is correlated with different immune subtypes but not with different cancer molecular subtypes. Further studies are needed to explore the mechanism of PRAF2 and cancer immunity in BC.

Single-cell transcriptomics data can be complemented by chromatin accessibility, surface protein expression, adaptive immune receptor repertoire profiling and spatial information. The increasing availability of single-cell data across modalities has motivated the development of novel computational methods to analyze derived biological insights [32]. In ovarian carcinoma (OV), the expression of PRAF2 was negatively associated with the cell cycle, differentiation, DNA repair and damage response, proliferation and invasion. In contrast, it was positively related to apoptosis, angiogenesis, hypoxia and quiescence. PRAF2 expression in uveal melanoma (UM) has a negative relationship with almost all tumor biological behaviors, including apoptosis, DNA damage and repair response, invasion and metastasis. Furthermore, previous studies has shown that PRAF2 expression is positively related to differentiation, EMT and apoptosis in acute myelocytic leukemia (AML). Our results demonstrated that PRAF2 is negatively correlated with cell apoptosis and inflammation but positively correlated with EMT. In Wu et al. study, they found that PRAF2 was a target gene of lncRNA(JHDM1D-AS1)/miR-450, reducing the level of PRAF2 in gastric cancer could significantly suppress cell invasion both in vitro and in vivo [33]. and Tamas and colleagues [34] found that downregulation of PRAF2 could significantly reduce the viability, migration and invasiveness of glioma cells. Interestingly, Wan et al. reported that PRAF2 also participated in regulating colorectal cancer cells via a non-EMT-dependent pathway [35]. Taken together, these results indicate that PRAF2 is a multifunctional factor involved in various cellular processes. Our next investigation was to explore

(See figure on next page.)

**Fig. 12** PRAF2 knockdown suppresses the proliferation, migration of BC cells in vitro and regulation of apoptosis related proteins. **A** Cell viability of BT-549 and MCF-7 cells following PRAF2 knockdown. **B** Wound healing assay of MCF-7 and BT-549 cells after transfection at 0 and 24 h. Scale bars, 100µm. **C** statistically significant difference in cells relative mobility was found between siRNA-NC and siRNA-PRAF2 BT-549 cells. **D** statistically significant difference in cells relative mobility was found between siRNA-NC and siRNA-PRAF2 MCF-7 cells. **E** Apoptosis related proteins expression was in MCF-7 、BT-549 cells transfected with siRNA-PRAF2 detected by Western blot analysis. **F** Quantitative analysis of expression of Bax 、Bcl-2 was in MCF-7 cell transfected with siRNA-PRAF2 detected by Western blot analysis. **G** Quantitative analysis of expression of Bax 、Bcl-2 was in BT-549 cell transfected with siRNA-PRAF2 detected by Western blot analysis. \*\*  $p < 0.01$ , \*\*\*  $p < 0.001$  \*\*\*\*  $p < 0.0001$

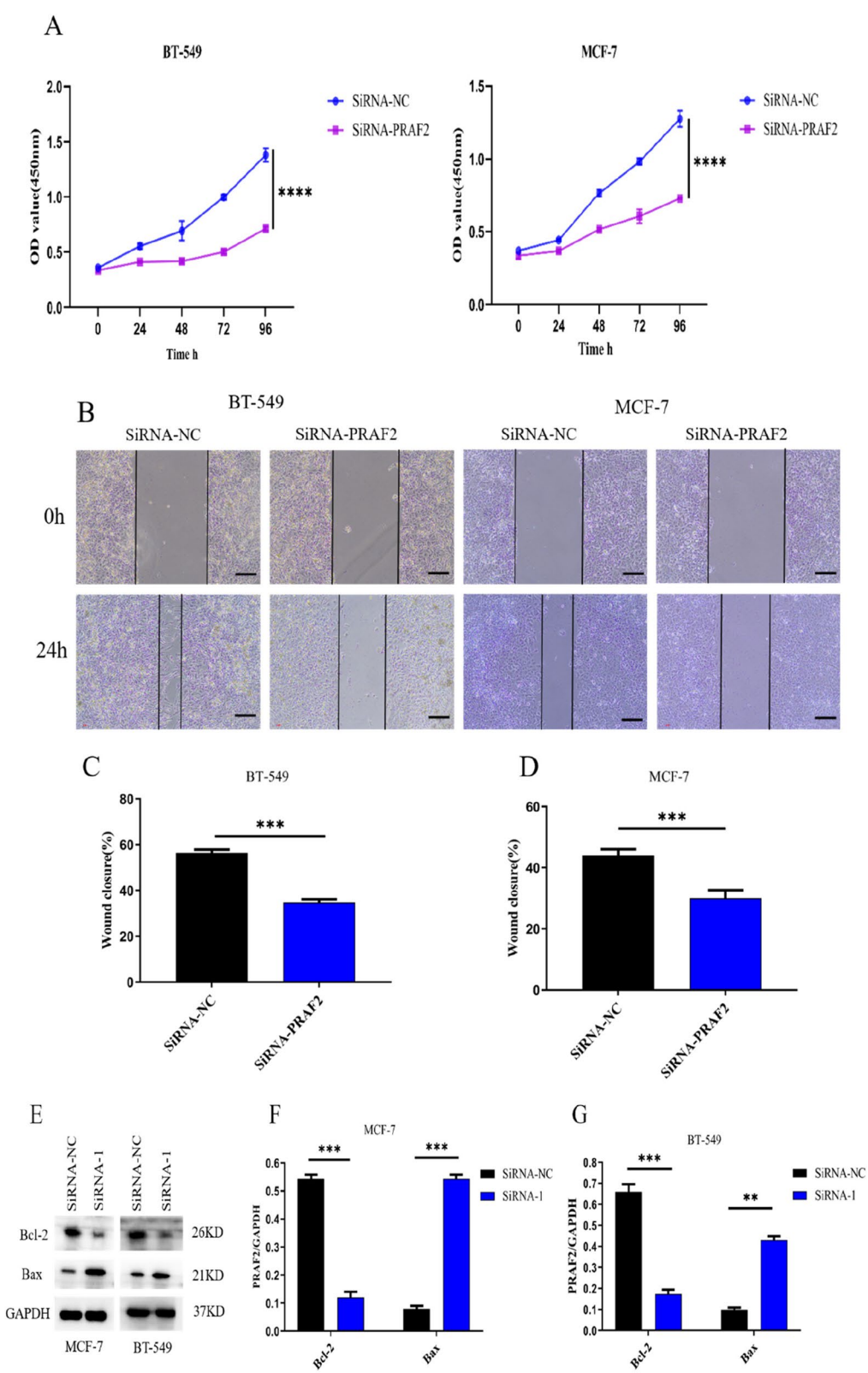


**Fig. 12** (See legend on previous page.)

related signaling pathways or genes of PRAF2. GO and KEGG analyses showed that PRAF2 is co-expressed with oxidative phosphorylation. Oxidative phosphorylation largely influences cancer cell viability. High oxidative phosphorylation is associated with worse outcomes. In TNBC, inhibiting oxidative phosphorylation could reverse chemotherapy resistance [36]. Ribosome biogenesis can promote tumor progression. Inhibition of ribosome biogenesis could improve oncological outcomes in different aspects, such as reducing tamoxifen resistance or enhancing chemotherapy effects [37, 38]. PRAF2 may interact with oxidative phosphorylation and ribosome biogenesis genes to promote BC.

Finally, we retrospectively analyzed PRAF2 expression from our institutional samples. The findings indicated that PRAF2 exhibits significant overexpression in BC in comparison to the adjacent healthy tissue. Subsequently, MCF-7 and BT-549 cells were employed for in vitro investigations. As expected, downregulation of PRAF2 in MCF-7 and BT-549 cells significantly reduced cell viability and migration as shown by CCK-8 and Wound healing assays. downregulation of PRAF2 presented pro-apoptotic proteins Bax was significantly higher, whereas, the anti-apoptotic protein Bcl-2 was significantly lower. We hope to further study the relevant mechanisms of PRAF2 in BC in the future.

## Conclusion

PRAF2 is highly expressed in various tumors and in BC. Clinical features are associated with PRAF2 expression. Higher expression of PRAF2 is related to poorer OS but not DFS. The expression of PRAF2 is associated with TILs and different immune subtypes. In single-cell analysis, PRAF2 was related to apoptosis, inflammation, EMT and hypoxia. PRAF2 is coexpressed with oxidative phosphorylation and ribosome biogenesis genes. Samples from our center showed higher expression of PRAF2 in BC. experiments validate inhibition of PRAF2 can reduce BC cell viability、migration and promoting cell apoptosis. PRAF2 may be a potential biomarker and therapeutic target for BC.

## Supplementary Information

The online version contains supplementary material available at <https://doi.org/10.1186/s12885-024-13258-7>.

Supplementary Material 1.

Supplementary Material 2.

Supplementary Material 3.

## Acknowledgements

Not applicable.

## Authors' contributions

The article was mainly written by Zheng Wang, Zilin Bi, Hongguang Bo and Junyi Xu and these authors contributed equally to the study. Zheng Wang, Zilin Bi, Hongguang Bo and Junyi Xu Research on Machine Learning. Rui Sha,Zhaocai Yin, Changsheng Yu and Bin Chen helped with data analysis and paper editing.Yufa Xu and Xiaomeng Shi, Wenbo Song did experimental study. The whole study was instructed by Yabing Wang, Qian Zhang and Jianping Chen. All authors reviewed and approved the manuscript.

## Funding

This work was supported by the Major scientific research project of Anhui Provincial Department of Education [grant number 2022AH040176], the key scientific research project of Anhui Provincial Department of Education [grant number 2024AH051951]. Teaching Quality and Reform Project of Wannan Medical College [grant number 2022jyxm60]. Teaching and Research Project of Anhui Provincial Department of Education [grant number 2023jyxm1220]. Key scientific research fund project of Wannan Medical College [grant number WK2022ZF17]. Anhui Provincial Health Commission "An Wei Lai" breast cancer Special Fund [grant number AHWJ2023BAb20032]. Anhui Provincial Health Commission Hengrui Innovative Drug Research Special Fund [grant number AHWJ2023BAc10053]. Research Foundation for Talents of Yijishan Hospital of Wannan Medical College [grant numbers YR202205, YR20220201]. Foundation for High-level Talents of Provincial Public Medical and Health Institutions [grant numbers GCCRC2022013, GCCRC2022018]. Health Commission of Tibet Autonomous Region Group Assistance Medical Research Fund project [grant number 20202531]. Fujian Natural Science Foundation Program [grant number 2021J01730]. Guiding project of Jiangsu Provincial Health Commission [grant number Z2021062]. Integrated development of universities and enterprises-HengRui Research Foundation [grant number XQHR202415]. Integrated development of universities and enterprises-QiLu Research Foundation [grant number XQQL202409].

## Data availability

The datasets used and/or analyzed during the current study are available from the corresponding author on reasonable request.

## Declarations

### Ethics approval and consent to participate

Informed consent to participate was obtained from all of the participants in the study. The study protocol was approved by the Ethics Committee of the Yijishan Hospital of Wannan Medical College (No. 202325).

### Consent for publication

Not applicable.

### Competing interests

The authors declare no competing interests.

Received: 24 February 2024 Accepted: 26 November 2024

Published online: 08 January 2025

## References

1. Xia C, Dong X, Li H, Cao M, Sun D, He S, et al. Cancer statistics in China and United States, 2022: profiles, trends, and determinants. *Chin Med J*. 2022;135(5):584–90.
2. Siegel RL, Miller KD, Wagle NS, Jemal A. Cancer statistics, 2023. *CA: Cancer J Clin*. 2023;73(1):17–48.
3. Joko-Fru WY, Miranda-Filho A, Soerjomataram I, Egue M, Akele-Akpo MT, N'da G, et al. Breast cancer survival in sub-Saharan Africa by age, stage at diagnosis and human development index: a population-based registry study. *Int J Cancer*. 2020;146(5):1208–18.
4. Schweneker M, Bachmann AS, Moelling K. JM4 is a four-transmembrane protein binding to the CCR5 receptor. *FEBS Lett*. 2005Mar 14;579(7):1751–8. <https://doi.org/10.1016/j.febslet.2005.02.037>.
5. Koomoa DL, Go RC, Wester K, Bachmann AS. Expression profile of PRAF2 in the human brain and enrichment in synaptic vesicles. *Neurosci Lett*.



- 2008May 9;436(2):171–6. <https://doi.org/10.1016/j.neulet.2008.03.030>. (Epub 2008 Mar 15).
6. Fo CS, Coleman CS, Wallick CJ, Vine AL, Bachmann AS. Genomic organization, expression profile, and characterization of the new protein PRA1 domain family, member 2 (PRAF2). *Gene*. 2006Apr 12;371(1):154–65. <https://doi.org/10.1016/j.gene.2005.12.009>. (Epub 2006 Feb 14).
7. Wang CH, Liu LL, Liao DZ, Zhang MF, Fu J, Lu SX, Chen SL, Wang H, Cai SH, Zhang CZ, Zhang HZ, Yun JP. PRAF2 expression indicates unfavorable clinical outcome in hepatocellular carcinoma. *Cancer Manag Res*. 2018Jul;25(10):2241–8. <https://doi.org/10.2147/CMAR.S166789>. PMID: 30100755.
8. Qian Z, Wei B, Zhou Y, Wang Q, Wang J, Sun Y, Gao Y, Chen X. PRAF2 overexpression predicts poor prognosis and promotes tumorigenesis in esophageal squamous cell carcinoma. *BMC Cancer*. 2019Jun 14;19(1):585. <https://doi.org/10.1186/s12885-019-5818-7>. PMID: 31200670.
9. Wang Y, Zhao Z, Jiao W, et al. PRAF2 is an oncogene acting to promote the proliferation and invasion of breast cancer cells. *Exp Ther Med*. 2022;24(6):738.
10. Thul PJ, Lindskog C. The human protein atlas: A spatial map of the human proteome. *Protein science : a publication of the Protein Society*. 2018;27(1):233–44.
11. Chandrashekar DS, Bashel B, Balasubramanya SAH, Creighton CJ, Ponce-Rodriguez I, Chakravarthi B, et al. UALCAN: A Portal for Facilitating Tumor Subgroup Gene Expression and Survival Analyses. *Neoplasia* (New York, NY). 2017;19(8):649–58.
12. Tang Z, Kang B, Li C, Chen T, Zhang Z. GEPIA2: an enhanced web server for large-scale expression profiling and interactive analysis. *Nucleic Acids Res*. 2019;47(W1):W556–60.
13. Cerami E, Gao J, Dogrusoz U, Gross BE, Sumer SO, Aksoy BA, Jacobsen A, Byrne CJ, Heuer ML, Larsson E, Antipin Y, Reva B, Goldberg AP, Sander C, Schultz N. The cBio cancer genomics portal: an open platform for exploring multidimensional cancer genomics data. *Cancer Discov*. 2012May;2(5):401–4.
14. Oates ME, Romero P, Ishida T, Ghalwash M, Mizianty MJ, Xue B, Dosztányi Z, Uversky VN, Obradovic Z, Kurgan L, Dunker AK, Gough J. D<sup>2</sup>P<sup>2</sup>: database of disordered protein predictions. *Nucleic Acids Res*. 2013;41(Database issue):D508–16.
15. Linding R, Jensen LJ, Diella F, Bork P, Gibson TJ, Russell RB. Protein disorder prediction: implications for structural proteomics. *Structure*. 2003Nov;11(11):1453–9.
16. Li T, Fu J, Zeng Z, Cohen D, Li J, Chen Q, et al. TIMER2.0 for analysis of tumor-infiltrating immune cells. *Nucleic Acids Res*. 2020;48(W1):W509–w14.
17. Ru B, Wong CN, Tong Y, Zhong JY, Zhong SSW, Wu WC, et al. TISIDB: an integrated repository portal for tumor-immune system interactions. *Bioinformatics* (Oxford, England). 2019;35(20):4200–2.
18. Yuan H, Yan M, Zhang G, Liu W, Deng C, Liao G, et al. CancerSEA: a cancer single-cell state atlas. *Nucleic Acids Res*. 2019;47(D1):D900–8.
19. Oughtred R, Rust J, Chang C, Breitkreutz BJ, Stark C, Willems A, et al. The BioGRID database: A comprehensive biomedical resource of curated protein, genetic, and chemical interactions. *Protein science : a publication of the Protein Society*. 2021;30(1):187–200.
20. Sherman BT, Hao M, Qiu J, Jiao X, Baseler MW, Lane HC, Imamichi T, Chang W. DAVID: a web server for functional enrichment analysis and functional annotation of gene lists (2021 update). *Nucleic Acids Res*. 2022Jul 5;50(W1):W216–21.
21. Livak KJ, Schmittgen TD. Analysis of relative gene expression data using real-time quantitative PCR and the 2(-Delta Delta C(T)) method. *Methods*. 2001;25:402–8.
22. Yoshihara K, Shahmoradgol M, Martínez E, Vegesna R, Kim H, Torres-Garcia W, et al. Inferring tumour purity and stromal and immune cell admixture from expression data. *Nat Commun*. 2013;4:2612.
23. Elhamamsy AR, Metge BJ, Alsheikh HA, Shevde LA, Samant RS. Ribosome Biogenesis: A Central Player in Cancer Metastasis and Therapeutic Resistance. *Cancer Res*. 2022;82(13):2344–53.
24. Yco LP, Geerts D, Koster J, Bachmann AS. PRAF2 stimulates cell proliferation and migration and predicts poor prognosis in neuroblastoma. *Int J Oncol*. 2013;42(4):1408–16.
25. Wang CH, Liu LL, Liao DZ, Zhang MF, Fu J, Lu SX, et al. PRAF2 expression indicates unfavorable clinical outcome in hepatocellular carcinoma. *Cancer management and research*. 2018;10:2241–8.
26. Geerts D, Wallick CJ, Koomoa DL, Koster J, Versteeg R, Go RC, et al. Expression of prenylated Rab acceptor 1 domain family, member 2 (PRAF2) in neuroblastoma: correlation with clinical features, cellular localization, and cerulenin-mediated apoptosis regulation. *Clinical cancer research : an official journal of the American Association for Cancer Research*. 2007;13(21):6312–9.
27. Adams S, Schmid P, Rugo HS, Winer EP, Loirat D, Awada A, et al. Pembrolizumab monotherapy for previously treated metastatic triple-negative breast cancer: cohort A of the phase II KEYNOTE-086 study. *Annals of oncology : official journal of the European Society for Medical Oncology*. 2019;30(3):397–404.
28. Loi S, Giobbie-Hurder A, Gombos A, Bachelot T, Hui R, Curigliano G, et al. Pembrolizumab plus trastuzumab in trastuzumab-resistant, advanced, HER2-positive breast cancer (PANACEA): a single-arm, multicentre, phase 1b–2 trial. *Lancet Oncol*. 2019;20(3):371–82.
29. Oshi M, Asaoka M, Tokumaru Y, et al. CD8 T Cell Score as a Prognostic Biomarker for Triple Negative Breast Cancer. *Int J Mol Sci*. 2020;21(18):6968.
30. Mehta AK, Kadel S, Townsend MG, Oliwa M, Guerriero JL. Macrophage Biology and Mechanisms of Immune Suppression in Breast Cancer. *Front Immunol*. 2021;12: 643771.
31. Hu D, Li Z, Zheng B, Lin X, Pan Y, Gong P, et al. Cancer-associated fibroblasts in breast cancer: Challenges and opportunities. *Cancer communications* (London, England). 2022;42(5):401–34.
32. Heumos L, Schaar AC, Lance C, et al. Best practices for single-cell analysis across modalities. *Nat Rev Genet*. 2023;24(8):550–72.
33. Wu M, Liu Y, Pu YS, Ma Y, Wang JH, Liu EQ. JHDM1D-AS1 aggravates the development of gastric cancer through miR-450a-2–3p-PRAF2 axis. *Life Sci*. 2021;265:118805. <https://doi.org/10.1016/j.lfs.2020.118805>. Epub 2020 Nov 24.
34. Borsics T, Lundberg E, Geerts D, Koomoa DL, Koster J, Wester K, et al. Subcellular distribution and expression of prenylated Rab acceptor 1 domain family, member 2 (PRAF2) in malignant glioma: Influence on cell survival and migration. *Cancer Sci*. 2010;101(7):1624–31.
35. He W, Tang J, Li W, Li Y, Mei Y, He L, et al. Mutual regulation of JAG2 and PRAF2 promotes migration and invasion of colorectal cancer cells uncoupled from epithelial-mesenchymal transition. *Cancer Cell Int*. 2019;19:160.
36. Evans KW, Yuca E, Scott SS, Zhao M, Paez Arango N, Cruz Pico CX, et al. Oxidative Phosphorylation Is a Metabolic Vulnerability in Chemotherapy-Resistant Triple-Negative Breast Cancer. *Can Res*. 2021;81(21):5572–81.
37. Erol A, Acikgoz E, Guven U, Duzagac F, Turkmani A, Colcimen N, et al. Ribosome biogenesis mediates antitumor activity of flavopiridol in CD44(+) / CD24(–) breast cancer stem cells. *Oncol Lett*. 2017;14(6):6433–40.
38. Tsoi H, You CP, Leung MH, Man EPS, Khoo US. Targeting Ribosome Biogenesis to Combat Tamoxifen Resistance in ER+ve Breast Cancer. *Cancers* (Basel). 2022;14(5):1251.

## Publisher's Note

Springer Nature remains neutral with regard to jurisdictional claims in published maps and institutional affiliations.